

Submicron-scale manipulation of phase separation in organic solar cells

Fang-Chung Chen, Yi-Kai Lin, and Chu-Jung Ko

Citation: *Applied Physics Letters* **92**, 023307 (2008); doi: 10.1063/1.2835047

View online: <http://dx.doi.org/10.1063/1.2835047>

View Table of Contents: <http://scitation.aip.org/content/aip/journal/apl/92/2?ver=pdfcov>

Published by the [AIP Publishing](#)

Articles you may be interested in

[Driving vertical phase separation in a bulk-heterojunction by inserting a poly\(3-hexylthiophene\) layer for highly efficient organic solar cells](#)

Appl. Phys. Lett. **98**, 023303 (2011); 10.1063/1.3541648

[Solution processed inverted tandem polymer solar cells with self-assembled monolayer modified interfacial layers](#)

Appl. Phys. Lett. **97**, 253307 (2010); 10.1063/1.3530431

[Electrical characterization of single-walled carbon nanotubes in organic solar cells by Kelvin probe force microscopy](#)

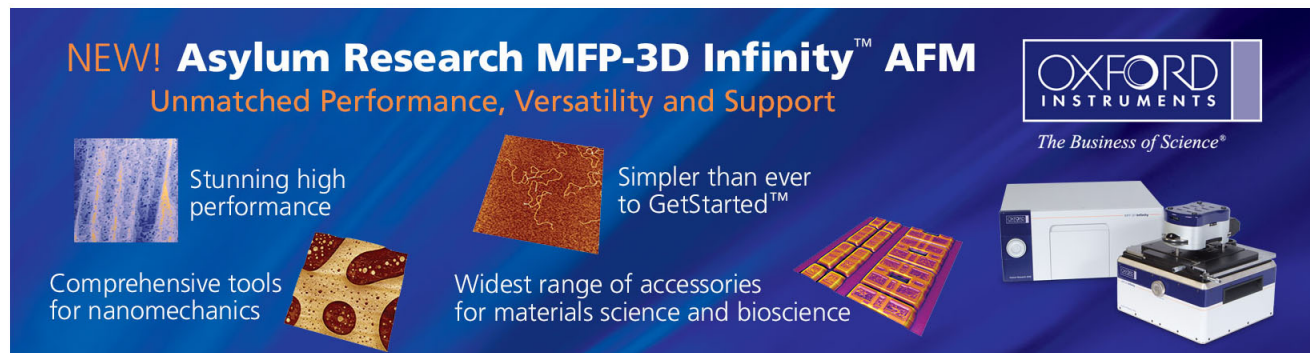
Appl. Phys. Lett. **96**, 083302 (2010); 10.1063/1.3332489

[The use of thermal initiator to make organic bulk heterojunction solar cells with a good percolation path](#)

Appl. Phys. Lett. **93**, 043304 (2008); 10.1063/1.2965468

[Photovoltaic enhancement of organic solar cells by a bridged donor-acceptor block copolymer approach](#)

Appl. Phys. Lett. **90**, 043117 (2007); 10.1063/1.2437100

The advertisement features a dark blue background with white and orange text. At the top left, it reads 'NEW! Asylum Research MFP-3D Infinity™ AFM' in large white letters, followed by 'Unmatched Performance, Versatility and Support' in orange. On the right, the 'OXFORD INSTRUMENTS' logo is shown in white, with the tagline 'The Business of Science®' below it. The central part of the ad contains four images with descriptive text: 1) A blue textured surface with the text 'Stunning high performance'. 2) A brown textured surface with the text 'Simpler than ever to GetStarted™'. 3) A yellow and red patterned surface with the text 'Comprehensive tools for nanomechanics'. 4) A white and blue AFM instrument with the text 'Widest range of accessories for materials science and bioscience'.

NEW! Asylum Research MFP-3D Infinity™ AFM
Unmatched Performance, Versatility and Support

OXFORD INSTRUMENTS
The Business of Science®

Stunning high performance

Simpler than ever to GetStarted™

Comprehensive tools for nanomechanics

Widest range of accessories for materials science and bioscience

Submicron-scale manipulation of phase separation in organic solar cells

Fang-Chung Chen^{a)} and Yi-Kai Lin

Department of Photonics, and Display Institute, National Chiao Tung University, Hsinchu, Taiwan 300, Republic of China

Chu-Jung Ko

Institute of Electro-optical Engineering, National Chiao Tung University, Hsinchu, Taiwan 300, Republic of China and National Nano Device Laboratories, Taiwan 300, Republic of China

(Received 12 November 2007; accepted 20 December 2007; published online 17 January 2008)

This paper describes a method for controlling the submicron-scale phase separation of poly(3-hexylthiophene) and (6,6)-phenyl-C₆₁-butyric acid methyl ester in organic solar cells. Using microcontact printing of self-assembled monolayers on the device buffer layer to divide the surface into two regimes having different surface energies, an interdigitated structure aligned vertical to the substrate surface is achieved after spontaneous surface-directed phase separation. The power conversion efficiency increases upon decreasing the grating spacing, reaching 2.47%. The hole mobility increased as a consequence of improved polymer chain ordering, resulting in higher device efficiency, while smaller pattern sizes were used. © 2008 American Institute of Physics.

[DOI: 10.1063/1.2835047]

Organic photovoltaic devices are receiving increasing attention because their favorable properties, such as light weight, fabrication at low temperature, low cost, and mechanical flexibility, are attractive for application in solar energy conversion.¹⁻⁴ The “bulk heterojunction” structure prepared through the blending of conjugated polymers and fullerenes is commonly used for preparing polymer photovoltaic cells on account of its simple device structure and ease of fabrication.¹⁻⁴ The two material phases form a randomly interpenetrating network having a large interfacial area that ensures the highly efficient dissociation of excitons. Because the separated electrons and holes must move through their two respective phases to the electrodes without significant recombination, the morphology of the polymer blend, which affects not only the charge separation but also the charge transportation, plays an important role in determining the device efficiency.

The ideal morphology would be one that is vertically separated with an average interspacial distance equal to or less than the exciton diffusion length. Furthermore, the interdigitated structure must be aligned perpendicular to the electrodes to provide direct pathways for efficient charge transportation.^{1,2} To achieve such an ideal structure, several groups have attempted to fabricate polymer solar cells with controllable vertical phase separation. Arias *et al.* reported that the use of organic solvents having high boiling points enhanced the vertical phase separation of a polymer mixture.⁵ In addition, Lindner *et al.* designed a block copolymer to control the phase separation vertically.⁶ More recently, Kim *et al.* used an imprint method to construct a submicron-scale ordered structure on a polymer thin film. Depositing the electron acceptor onto the artificial structure led to vertical interpenetrative phase separation.⁷ In this paper, we report an effective method for inducing self-organized phase separation in polymer photovoltaic devices. We obtained an interdigitated structure vertical to the substrate surface through spontaneous phase separation directed

by patterning the device buffer layer, using microcontact printing (μ CP), into two regimes having different surface energies.

Figure 1 presents the process flow of this approach. Polydimethylsiloxane (PDMS) (Sygard184) was used as the mold to transfer the pattern. The patterns on the PDMS molds, including grating sizes of 1.0, 0.75, and 0.5 μ m, were transferred from silicon wafers, which were fabricated using standard semiconductor processes. Using μ CP, the PDMS mold defined a patterned area of a self-assembled monolayer (SAM) prepared from 3-aminopropyltriethoxysilane (APTES) on a layer of poly(3,4-ethylenedioxythiophene):poly(styrenesulfonate) (PEDOT:PSS), which had been deposited on the indium tin oxide (ITO) substrate. Before μ CP, the PEDOT:PSS was pretreated with UV ozone for 15 min and some dangling bonds of oxygen were, therefore, produced on the surface. When aminosilane contacted with the oxidized surface, the SAM molecules were spontaneously linked onto the surface via a dehydration reaction. For the preparation of the active layer, poly(3-hexylthiophene) (P3HT) and (6,6)-phenyl-C₆₁-butyric acid methyl ester (PCBM) (1:1, w/w) were dissolved in 1,2,4-trichlorobenzene. The solution were spin coated at 600 rpm on the SAMs patterned PEDOT:PSS layer.

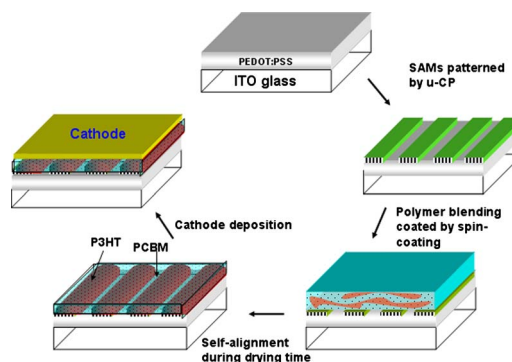


FIG. 1. (Color online) Fabrication processes of polymer solar cells in this study.

^{a)}Electronic mail: fchen@mail.nctu.edu.tw.

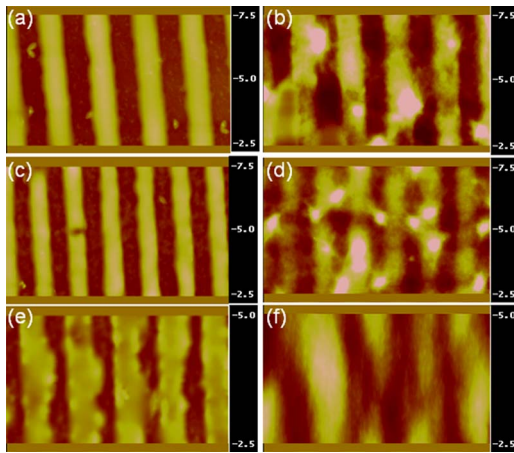


FIG. 2. (Color online) Tapping mode AFM images of the SAM-patterned PEDOT:PSS films [(a), (c), and (e)] and the P3HT:PCBM films on the SAM-patterned PEDOT:PSS [(b), (d), and (f)]. The grating sizes were $1.00 \mu\text{m}$ in (a) and (b), $0.75 \mu\text{m}$ in (c) and (d), and $0.50 \mu\text{m}$ in (e) and (f).

The thickness of the active layer was $260 \pm 10 \text{ nm}$. After spin coating, the active layer was spontaneously dried in a covered Petri dish for 20 min to induce lateral phase separation.⁴ Then, the polymer film was heated at $110 \text{ }^\circ\text{C}$ for 15 min to remove the residue solvent. Finally, Al and Ca were deposited on the active layer as the cathode and the whole device was placed in a glove box filled with nitrogen gas. The dark and light current density-voltage (J - V) curves were measured using a Keithley 2400 source meter. The photocurrent was obtained under illumination from a Thermal Oriel solar simulator (AM1.5G). The illumination intensity was calibrated using a standard Si photodiode detector equipped with a KG-5 filter.⁸

The SAM grating pattern on the PEDOT:PSS layer were firstly examined by using atomic force microscopy (AFM). Figures 2(a)–2(d) display SAM patterns of varying sizes. When the grating size was $0.5 \mu\text{m}$, the edge of the grating was slightly unclear as a result of defects in the template. After coating the P3HT/PCBM blend on the patterned surface, phase separation clearly occurred following the grating pattern after solvent annealing [cf. Figs. 2(b), 2(d), and 2(e)]. Unlike the conventional phase separation of P3HT and PCBM which is usually controlled through thermal treatment or solvent evaporation,^{3,4} the phase separation induced by the underlying pattern occurs through a process known as pattern-directed spinodal decomposition.⁹ Driven by the two different surface free energies presented on the buffer PEDOT:PSS layer, the two phases adhered spontaneously and selectively onto their preferred individual surfaces.

Several authors have reported that spinodal decomposition occurs efficiently in polymer-blend films on SAM-patterned surfaces.^{9–11} We note that well-defined phase separation in our system occurred only after manipulation of the SAM pattern. Furthermore, we utilized scanning electron microscopy to examine the variations in thickness of the P3HT and PCBM thin films while dipping the patterned substrates into the solutions. We found that P3HT adhered favorably onto the APTES surface pattern rather than on the PEDOT:PSS surface. In contrast, the adhesion of PCBM on the SAM-patterned surface was quite limited. Thus, we infer that the P3HT-rich regime was located on the APTES-patterned areas and the PCBM-rich phase on the exposed PEDOT:PSS.

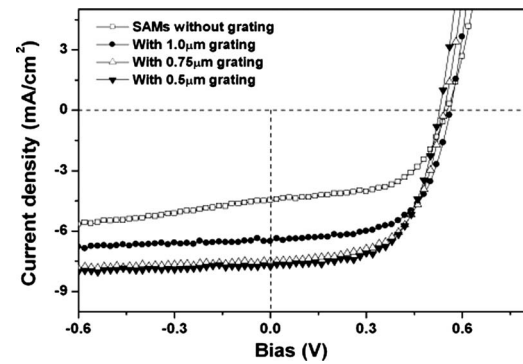


FIG. 3. Current density vs voltage (J - V) characteristics of the devices with various SAM-patterned grating sizes measured under illumination (simulated AM1.5G, 100 mW cm^{-2}).

Figure 3 displays the J - V characteristics of the PV devices incorporating the various grating patterns. The device efficiency increased upon decreasing the grating size. Each device had a similar open-circuit voltage (V_{oc}). The device covered with the SAM without patterning exhibited poor performance. The calculated power conversion efficiency (PCE) was 1.43%. When using grating diameters of 1.00 and $0.75 \mu\text{m}$, the values of the PCE increased to 2.22% and 2.41%, respectively. At a grating spacing of $0.5 \mu\text{m}$, the values of J_{sc} and PCE improved to 7.76 mA/cm^2 and 2.47%, respectively. Figure 3 provides a summary of the overall device performance with respect to the grating period. We observe that the short circuit current density increased upon decreasing the grating spacing.

To determine the effect on the film internal resistance respect of the grating spacing, we derived device series resistances (R_s) from the slopes of the J - V curves obtained in the dark.^{12,13} We found that the series resistance gradually reduced from 3.21 to $3.04 \Omega \text{ cm}^2$ when the grating size decreased from 1.00 to $0.50 \mu\text{m}$. The nonpatterned device had an even larger resistance. The major contributions to the value of R_s include the bulk resistance ($R_{s,bulk}$) and the contact resistance ($R_{s,contact}$). The value of $R_{s,contact}$ originates from the interface between the electrodes and the active layer. The value of $R_{s,bulk}$ arises from the bulk resistance of the organic layers (P3HT:PCBM blends and PEDOT:PSS) and the electrodes (ITO and cathode metals). Because the contact area at the electrodes was similar in each device, the value of $R_{s,contact}$ was constant, irrespective of the grating size. Therefore, any series resistance variation probably arose from the reduction of the bulk resistance. Consequently, we infer that our polymer chains became more ordered when the smaller grating size was used.

To further characterize the thin film morphologies, we extracted the values of the hole mobilities from the current density-voltage characteristics of the hole-only devices in the dark [Fig. 4(a)].¹⁴ We fabricated these devices using a high-work-function material, molybdenum oxide (MoO_3), as the buffer layer at the cathode to block the injection of electrons. The hole mobility was calculated at the regime of the space-charge-limited current regime according to the equation¹⁴

$$J = 9\epsilon_0\epsilon_p\mu V^2/8L, \quad (1)$$

where $\epsilon_0\epsilon_p$ is the permittivity of the polymer, μ is the carrier mobility, and L is the device thickness. From Fig. 4(a), we know that the hole mobility of the device prepared without

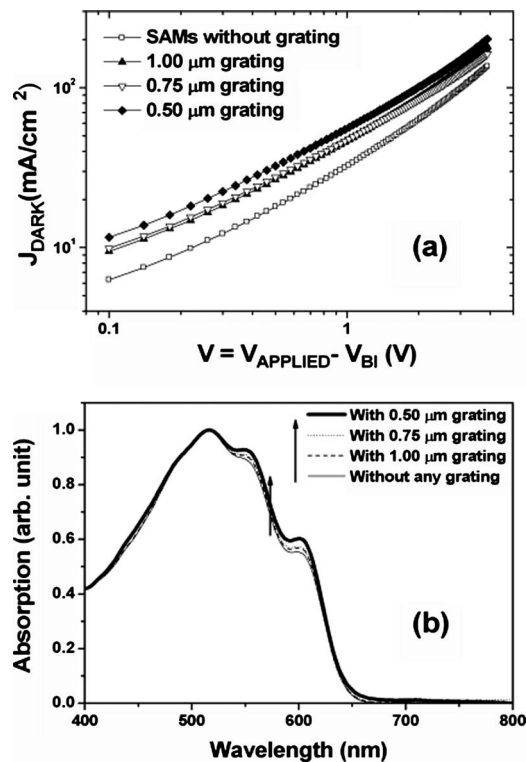


FIG. 4. (a) Dark J - V curves of the hole-only devices with various grating sizes. (b) The UV-vis spectrum of the P3HT:PCBM films on PEDOT:PSS patterned with different grating sizes.

SAM patterning was $2.53 \times 10^{-8} \text{ m}^2/\text{V s}$. On the other hand, for the devices prepared with grating sizes of 1.00, 0.75, and $0.50 \mu\text{m}$, the mobilities increased to 3.94×10^{-8} , 4.10×10^{-8} , and $4.23 \times 10^{-8} \text{ m}^2/\text{V s}$, respectively. The increased hole mobility observed upon reducing the grating size suggests that patterning the SAMs through contact printing helps to align the P3HT phase.

It has been reported that the presence of PCBM in P3HT hampers the crystallization of the polymer.¹⁵ In our device prepared using the larger grating pattern, although phase separation occurred, the two components did not segregate perfectly. Even though PCBM has very high diffusivity in P3HT, some PCBM remained in the P3HT-rich domain prior to solidification of the films. In contrast, when we used the smaller grating size, both molecules had a shorter distance for diffusion. As a result, the degree of phase separation was more complete. In other words, the amount of PCBM in the P3HT-rich domain was lower for the film blend when the grating size was shorter. Consequently, we believed that P3HT aligned in a more orderly manner in the devices containing the smaller grating size.

To confirm this hypothesis, we examined the absorption spectra of the P3HT:PCBM films patterned on the

PEDOT:PSS layer at various grating sizes as Fig. 4(b). In all cases, we clearly observe vibronic features arising from P3HT.¹⁶ Furthermore, the absorption shoulders became more pronounced upon decreasing the grating size. These results are consistent with the improved hole mobility. Both phenomena suggest that the patterned SAMs assisted with the organization of the main chains and reduced the presence of irregularities in the blend film. Hence, improved π - π stacking enhanced the charge mobility.

In summary, we have utilized SAM patterning to control the phase separation of P3HT and PCBM in a film blend on the path to fabricating polymer solar cells. With a smaller pattern size, the two-component phase separation occurred more effectively. Because the presence of PCBM hampers the alignment of P3HT, the polymer chains became more ordered when the distance for diffusion became shorter, leading to better phase separation. We suggest that the hole mobility increased because of improved π - π stacking of the polymer chains on the patterned PEDOT:PSS, resulting in higher device efficiency.

We thank the National Science Council (NSC-95-2221-E-009-305 and NSC-96-ET-7-009-001-ET) and the MOE ATU program for financial support.

- ¹K. M. Coakley and M. D. McGehee, *Chem. Mater.* **16**, 4533 (2004).
- ²S. Gunes, H. Neugebauer, and N. S. Sariciftci, *Chem. Rev. (Washington, D.C.)* **107**, 1324 (2007).
- ³W. L. Ma, C. Y. Yang, X. Gong, K. Lee, and A. J. Heeger, *Adv. Funct. Mater.* **15**, 1617 (2005).
- ⁴G. Li, V. Shrotriya, J. S. Huang, Y. Yao, T. Moriarty, K. Emery, and Y. Yang, *Nat. Mater.* **4**, 864 (2005).
- ⁵A. C. Arias, N. Corcoran, M. Banach, R. H. Friend, J. D. MacKenzie, and W. T. S. Huck, *Appl. Phys. Lett.* **80**, 1695 (2002).
- ⁶S. M. Lindner, S. Huttner, A. Chiche, M. Thelakkat, and G. Krausch, *Angew. Chem., Int. Ed.* **45**, 3364 (2006).
- ⁷M. S. Kim, J. S. Kim, J. C. Cho, M. Shtein, L. J. Guo, and J. Kim, *Appl. Phys. Lett.* **90**, 123113 (2007).
- ⁸V. Shrotriya, G. Li, Y. Yao, T. Moriarty, K. Emery, and Y. Yang, *Adv. Funct. Mater.* **16**, 2016 (2006).
- ⁹A. Karim, J. F. Douglas, B. P. Lee, S. C. Glotzer, J. A. Rogers, R. J. Jackman, E. J. Amis, and G. M. Whitesides, *Phys. Rev. E* **57**, R6273 (1998).
- ¹⁰J. K. Cox, A. Eisenberg, and R. B. Lennox, *Curr. Opin. Colloid Interface Sci.* **4**, 52 (1999).
- ¹¹P. Cyganik, A. Bernasik, A. Budkowski, B. Bergues, K. Kowalski, J. Rysz, J. Lekki, and M. Lekka, *Vacuum* **63**, 307 (2001).
- ¹²W. D. Johnston, Jr., *Solar Voltaic Cells* (Dekker, New York, 1980).
- ¹³D. W. Sievers, V. Shrotriya, and Y. Yang, *J. Appl. Phys.* **100**, 114509 (2006).
- ¹⁴V. Shrotriya, Y. Yao, G. Li, and Y. Yang, *Appl. Phys. Lett.* **89**, 063505 (2006).
- ¹⁵A. Swinnen, I. Haeldermans, M. Vande Ven, J. D'Haen, G. Vanhoyland, S. Aresu, M. D'Olieslaeger, and J. Manca, *Adv. Funct. Mater.* **16**, 760 (2006).
- ¹⁶M. Sundberg, O. Inganäs, S. Stafstrom, G. Gustafsson, and B. Sjogren, *Solid State Commun.* **71**, 435 (1989).